JOURNAL OF GUIDANCE, CONTROL, AND DYNAMICS
Vol. 17, No. 2, March–April 1994

Range Optimal Trajectories for an Aircraft Flying in the Vertical Plane

Hans Seywald*
Analytical Mechanics Associates, Inc., Hampton, Virginia 23666
Eugene M. Cliff†
Virginia Polytechnic Institute and State University, Blacksburg, Virginia 24061
and
Klaus H. Well‡
University of Stuttgart, D-7000 Stuttgart, Germany

Range optimal trajectories for an aircraft flying in the vertical plane are obtained from Pontryagin's minimum principle. Control variables are the load factor, which appears nonlinearly in the equations of motion, and the throttle setting, which appears only linearly. Both controls are subject to fixed bounds. Additionally, a dynamic pressure limit is imposed, which represents a first-order state-inequality constraint. For fixed flight time, initial coordinates, and final coordinates of the trajectory, the effect of the load factor limit on the resulting optimal switching structure is studied. All trajectories involve singular control along arcs with active dynamic pressure limit. For large flight times the optimal switching structures have not yet been found.

I. Introduction

GREAT efforts are being undertaken to develop real-time, near-optimal feedback algorithms either for enhancement of aircraft performance by optimizing specified maneuvers or as autonomous guidance schemes for short- and medium-range air-to-air missiles.[1-5] Open-loop control logics obtained by state-of-the-art optimization techniques are an important tool in testing the accuracy and finding the limits of such feedback laws. In a recent study[6,7] open-loop optimal control solutions in conjunction with perturbation techniques have been used directly to develop feedback algorithms. In this context minimum-time intercept trajectories, or, often equivalently, maximum-range trajectories for fixed flight time play an important role in modern air combat scenarios.

In the present paper Pontryagin's minimum principle (PMP)[8-10] is applied to determine range optimal trajectories for an aircraft flying in the vertical plane. State variables are energy E, altitude h, and flight-path angle γ; control variables are load factor n and throttle setting η. Control η appears only linearly in the equations of motion and is subject to fixed bounds $0 \le \eta \le 1$. Additionally, a dynamic pressure limit is imposed on the trajectory, which in the context of optimal control represents a first-order state inequality constraint.

For sufficiently large fixed final times a good approximation to the maximum-range trajectory can be obtained by breaking the flight into three phases: 1) climb to the dash-point, 2) steady-state cruise at the dash-point, and 3) final transient to reach the terminal constraints. The dash-point is the point of maximum sustainable speed on the level-flight envelope. The associated state values can be found by solving the maximization problem

$$\max_{E,\,h,\,\gamma;\,n,\,\eta} \quad v,\ v = \sqrt{2g(E-h)}$$

subject to the level-flight constraints

$$\gamma = 0$$

$$\dot{\gamma} = 0$$

$$\dot{E} = 0$$

and the control constraints for n and η.

In the present paper we consider trajectories that start at the dash-point. The final conditions are chosen rather arbitrarily, but such that the aircraft is forced to dive to lower altitudes at final time. Furthermore, the final energy/altitude pair is located inside the level-flight envelope and off the dynamic pressure limit.

For fixed boundary conditions and fixed flight time we study the effect of the load factor limit $|n| \le n_{\max}$ on the structure of the optimal solution. Six different switching structures involving singular control on state constrained arcs are encountered if $n_{\max}$ is varied between $n_{\max} = \infty$ and $n_{\max} = 5$. The switching structures identified in this paper appear to be of a general nature and are not restricted to the specific boundary conditions considered here. However, for the boundary conditions prescribed in this paper, the structure of the optimal solution has not yet been found for flight times greater than 62 s.

II. Aircraft Model

The equations of motion of an aircraft flying in the vertical plane are

$$\dot{E} = (\eta T - D)\frac{v}{W} \tag{1}$$

$$\dot{h} = v \sin\gamma \tag{2}$$

$$\dot{\gamma} = \frac{g}{v}\left(\frac{L}{W} - \cos\gamma\right) \tag{3}$$

$$\dot{x} = v \cos\gamma \tag{4}$$

The specific energy E, replacing velocity v, the altitude h, the flight-path angle γ, and the range x are the state variables. Load factor n and the power setting η are the control vari-

Received Dec. 2, 1992; revision received June 7, 1993; accepted for publication June 8, 1993.

*Supervising Engineer, 17 Research Drive; working under contract at the Spacecraft Controls Branch, NASA-LARC. Member AIAA.
†Reynolds Metals Professor, Interdisciplinary Center for Applied Mathematics. Fellow AIAA.
‡Professor, Institute for Flight Mechanics and Control, Sorststrasse 86. Fellow AIAA.

ables. The mass m of the vehicle and the gravitational acceleration g are assumed to be constant, namely

$$m = 16818 \text{ kg}$$

$$g = 9.80665 \text{ m/s}^2$$

The vehicle weight is given by $W = mg$. Velocity v is a short notation for $v = \sqrt{2g(E-h)}$. The air density ρ in kilograms per meter^3 is given by

$$\rho(h) = 1.225\, e^{y}$$

$$y = -0.12122693\ 10^{-3}\, h + r - 1.0228055$$

$$r = 1.0228055\, e^{-z}$$

$$z = -3.48643241\ 10^{-5}\, h + 3.50991865\ 10^{-9}\, h^2$$

$$+ -8.33000535\ 10^{-14}\, h^3 + 1.15219733\ 10^{-18}\, h^4$$

The speed of sound in meters per second is given by

$$a(h) = 20.0468\sqrt{\theta}$$

where the temperature θ is given by

$$\theta = 292.1 - 8.87743\ 10^{-3}\, h + 0.193315\ 10^{-6}\, h^2 + 3.72\ 10^{-12}\, h^3$$

In these expressions h is altitude in meters. The Mach number is given by $M = v/a(h)$. The lift L, the drag D, and the maximum thrust T in Newtons, respectively, are given as functions of h, M, and n

$$q = \tfrac{1}{2}\rho(h)v^2S$$

$$L = Wn$$

$$D = q\left(C_{D0}(M) + K(M)\frac{W^2}{q^2}n^2\right)$$

$$C_{D0} = \frac{a_4M^4 + a_3M^3 + a_2M^2 + a_1M + a_0}{b_4M^4 + b_3M^3 + b_2M^2 + b_1M + b_0}$$

$$K = \frac{c_4M^4 + c_3M^3 + c_2M^2 + c_1M + c_0}{d_5M^5 + d_4M^4 + d_3M^3 + d_2M^2 + d_1M + d_0}$$

$$T(h, M) = e_5(M)h^5 + e_4(M)h^4 + e_3(M)h^3 + e_2(M)h^2$$

$$+ e_1(M)h + e_0(M)$$

where for $i = 0, 1, \ldots, 5$

$$e_i(M) = (f_{i5}M^5 + f_{i4}M^4 + f_{i3}M^3 + f_{i2}M^2 + f_{i1}M + f_{i0})$$

The numerical values of the constants a_i, b_i, c_i, d_i, and f_{ij} are given in Tables 1-3 and represent a high performance fighter-interceptor.

III. Problem Formulation

The problem under consideration is that of finding control functions $\eta(t)$ and $n(t)$ that steer an aircraft from prescribed initial states: energy E_0, altitude h_0, and flight-path angle γ_0 to prescribed final states: energy E_f, altitude h_f, and flight-path angle γ_f in prescribed flight time $(t_f - t_0)$ (without loss of generality $t_0 = 0$) such that the downrange x is maximized. Along the optimal trajectory a set of state and control constraints has to be satisfied. Explicitly the problem can be stated in Mayer form as follows:

$$\min -x(t_f) \tag{5}$$

subject to the state equations (1-4), the control constraints

$$-\eta \le 0 \tag{6}$$

$$\eta - 1 \le 0 \tag{7}$$

$$-n - n_{\max} \le 0 \tag{8}$$

$$+n - n_{\max} \le 0 \tag{9}$$

the state constraint

$$C_0(E, h, \gamma, x) := v - v_{\max}(h) \le 0 \tag{10}$$

and the boundary conditions

$$E(0) = 38029.207 \text{ m} \tag{11a}$$

$$h(0) = 12119.324 \text{ m} \tag{11b}$$

$$\gamma(0) = 0 \text{ rad} \tag{11c}$$

$$x(0) = 0 \text{ m} \tag{11d}$$

$$E(t_f) = 9000 \text{ m} \tag{11e}$$

$$h(t_f) = 942.292 \text{ m} \tag{11f}$$

$$\gamma(t_f) = -0.2 \text{ rad} \tag{11g}$$

$$x(t_f) \text{ to be optimized} \tag{11h}$$

and the final time t_f prescribed, e.g.,

$$t_f = 60 \text{ s} \tag{12}$$

Table 1 Coefficients for C_{D0}-model

i	a_i		b_i	
0	−2.61059846050	10^{-2}	+7.29821847445	10^{-1}
1	+8.57043966269	10^{-2}	−3.25219000620	10^{0}
2	+1.07863115049	10^{-1}	+5.72789877344	10^{0}
3	−6.44772018636	10^{-2}	−4.57116286752	10^{0}
4	+1.64933626507	10^{-2}	+1.37368651246	10^{0}

Table 2 Coefficients for K-model

i	c_i		d_i	
0	+1.23001735612	10^{0}	+1.42392902737	10^{+1}
1	−2.97244144190	10^{0}	−3.24759126471	10^{+1}
2	+2.78009092756	10^{0}	+2.96838743792	10^{+1}
3	−1.16227834301	10^{0}	−1.33316812491	10^{+1}
4	+1.81868987624	10^{-1}	+2.87165882405	10^{+1}
5	—		−2.27239723756	10^{-1}

Table 3 Coefficients for thrust model

i	$f_{ij}, j=0$	$f_{ij}, j=1$	$f_{ij}, j=2$
0	+0.11969995703 10^{6}	−0.35217318620 10^{6}	+0.60452159152 10^{6}
1	−0.14644656421 10^{5}	+0.51808811078 10^{5}	−0.95597112936 10^{5}
2	−0.45534597613 10^{3}	+0.23143969006 10^{4}	−0.38860323817 10^{4}
3	+0.49544694509 10^{3}	−0.22482310455 10^{4}	+0.39771922607 10^{4}
4	−0.46253181596 10^{2}	+0.20894683419 10^{3}	−0.36835984294 10^{3}
5	+0.12000480258 10^{1}	−0.53807416658 10^{1}	+0.94529288471 10^{1}
i	$f_{ij}, j=3$	$f_{ij}, j=4$	$f_{ij}, j=5$
0	−0.43042985701 10^{6}	+0.13656937908 10^{6}	−0.16647992124 10^{5}
1	+0.83271826575 10^{5}	−0.32867923740 10^{5}	+0.49102536402 10^{4}
2	+0.12357128390 10^{4}	+0.55572727442 10^{3}	−0.23591380327 10^{3}
3	−0.30734191752 10^{4}	+0.10635494768 10^{4}	−0.13626703723 10^{3}
4	+0.29388870979 10^{3}	−0.10784916936 10^{3}	+0.14880019422 10^{2}
5	−0.76204728620 10^{1}	+0.28552696781 10^{1}	−0.40379767869 10^{0}

Here n_{max} is a specified constant denoting the maximum allowed absolute value of the load factor $n = L/W$. In state constraint Eq. (10) $v_{max}(h)$ is a specified function of altitude h. With $v_{max}(h)$ chosen appropriately, this covers the important case of a dynamic pressure constraint. Boundary conditions (11a–11c) refer to the dash-point or high speed point. The boundary conditions (11e–11g) are picked more or less arbitrarily. The only important features are that $h(t_f) < h(0)$ and $v(t_f) = \sqrt{2g(E(t_f) - h(t_f))} < v_{max}(h(t_f))$, i.e., in the altitude-velocity chart the prescribed final point of the trajectory is located to the left of the state constraint (10).

IV. Relaxed Problem Formulation

Existence theorems in optimal control theory require convexity of a certain velocity set or hodograph.[9] Given a state equation $\dot{x} = f(x, u)$, $x \in \boldsymbol{R}^n$, $u \in \boldsymbol{R}^m$ with admissible controls $u \in U \subset \boldsymbol{R}^m$, the hodograph at some fixed state $x_0 \in \boldsymbol{R}^n$ is defined as the set $S = \{\dot{x} \in \boldsymbol{R}^n | \dot{x} = f(x_0, u), u \in U\}$ of possible state rates. For state equations (1–4) with controls $[\eta, n] \in \boldsymbol{R}^2$ subject to the constraints equations (6–9), the hodograph is clearly nonconvex as indicated in Fig. 1. This nonconvexity results from the fact that with throttle $\eta = 0$ the smallest energy rate (= the largest negative energy rate) can be achieved only for $n = \pm n_{max}$. If, for example, an optimal control problem is formulated such that along some time interval the aircraft is required to dissipate energy at maximum rate while keeping the flight-path angle constant, then a near-optimal solution would be achieved by setting $\eta = 0$ and by rapidly switching the load factor between $n = \pm n_{max}$ such that, in the average, $\dot{\gamma} = 0$ is achieved. In the limit the optimal solution would be achieved only by letting the load factor n chatter at an infinite rate. However, this limiting process is not well-defined in the sense that the limit load factor function of time is not Lebesgue integrable, and hence is not an admissible controller. Strictly speaking, a solution does not exist in this case for the problem at hand. It may be desirable, however, to determine the solution associated with the limiting case of chattering control. To do this it is necessary to convexize the hodograph. That means one has to add to the set of admissible state rates all those state rates that are located along straight lines in between any two admissible state rates of the original hodograph. For aircraft models with quadratic drag polar, such as the one used in this paper, this can be achieved by rewriting state equation (1) as

$$\dot{E} = [\delta(T - D + D_{max}) - D_{max}] \frac{v}{W} \tag{13}$$

with

$$D_{max}(M, h) := D(M, h, n_{max})$$

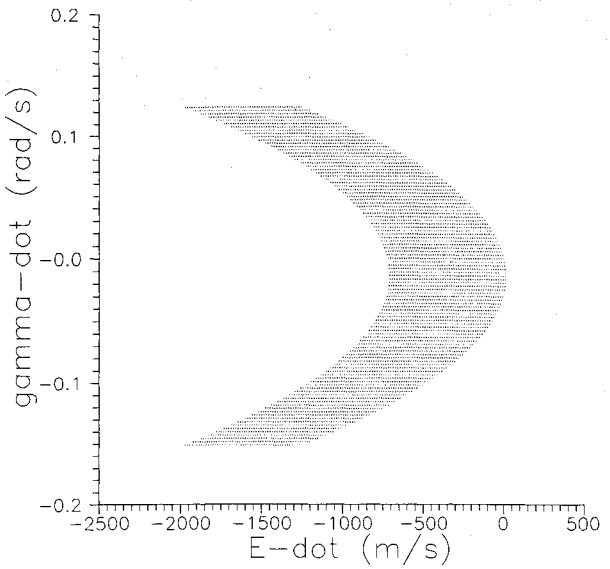

Fig. 1 Hodograph for unrelaxed problem.

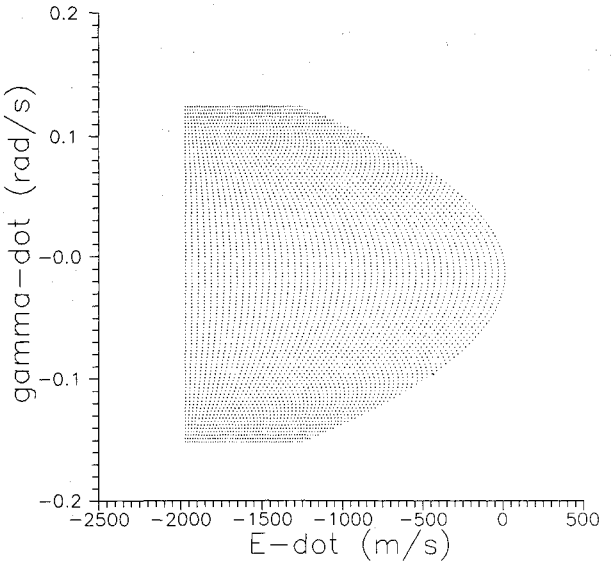

Fig. 2 Hodograph for relaxed problem.

The new control δ replaces the old control η and is subject to the constraints

$$-\delta \le 0 \tag{14}$$

$$\delta - 1 \le 0 \tag{15}$$

Of course, the control δ is rather artificial and lacks the physical meaning of a throttle parameter. It should be noted, however, that generally in optimal control the controls only play the role of bookkeeping parameters used to parameterize the set of admissible state rates. This arbitrariness of the controls becomes more clear by noting that under control transformations that leave the hodograph unchanged, the state and state rate functions of time associated with the optimal solution remain unchanged, whereas the optimal control function of time may become completely different.

To summarize, the relaxed control problem, which is used for the remainder of this paper, is given by

$$\min -x(t_f)$$

subject to the state equations (13) and (2–4), control constraints (14), (15), (8), and (9), state constraint (10), boundary conditions (11a–11g), and the final time t_f prescribed as in Eq. (12). That the hodograph of the relaxed dynamical system is equal to the convex hull of the hodograph of the original dynamical system can be seen by direct comparison (see Figs. 1 and 2). For the present problem, both hodographs can be constructed analytically by first determining the respective boundaries [by sequentially setting $\eta = 0$, $\eta = 1$, $n = -n_{max}$, and $n = +n_{max}$ in Eqs. (13) and (2–4), and $\delta = 0$, $\delta = 1$, $n = -n_{max}$, and $n = +n_{max}$ in Eqs. (14), (15), (8), and (9)] and then noting that all points in the interior of these boundaries also belong to the respective hodograph.

The state inequality constraint (10) being active on some time interval $[\tau_1, \tau_2]$ {i.e., $C_0(E, h, \gamma, x) \equiv 0$ on $[\tau_1, \tau_2]$} is equivalent to

$$C_0(E, h, \gamma, x) \equiv 0 \quad \text{at} \quad t = \tau_1 \tag{16}$$

$$C_1(E, h, \gamma, x; n, \delta) \equiv 0 \quad \text{on} \quad [\tau_1, \tau_2] \tag{17}$$

where

$$C_1(E, h, \gamma, x; n, \delta) := \frac{d}{dt} C_0(E, h, \gamma, x)$$

$$= [\delta(T - D + D_{max}) - D_{max}]g/W - v \sin \gamma(v'_{max} + g/v) \tag{18}$$

V. Minimum Principle

The relaxed optimization problem as stated earlier is solved by applying the PMP.[8-10] The PMP requires that at every point in time the controls are to be chosen such that the variational Hamiltonian

$$H(E, h, \gamma, x, \lambda_E, \lambda_h, \lambda_\gamma, \lambda_x, \delta, n) = \lambda_E \dot{E} + \lambda_h \dot{h} + \lambda_\gamma \dot{\gamma} + \lambda_x \dot{x} \tag{19}$$

is minimized subject to all control constraints. Let the vector valued function $g : \boldsymbol{R}^6 \mapsto \boldsymbol{R}^4$ be defined by

$$\begin{aligned} g_1(E, h, \gamma, x; \delta, n) &= -\delta \\ g_2(E, h, \gamma, x; \delta, n) &= \delta - 1 \\ g_3(E, h, \gamma, x; \delta, n) &= -n - n_{\max} \\ g_4(E, h, \gamma, x; \delta, n) &= +n - n_{\max} \end{aligned} \tag{20}$$

so that inequalities (14), (15), (8), and (9) can be written concisely as $g \le 0$. Then Lagrange multipliers λ_E, λ_h, λ_γ, and λ_x are solutions of the adjoint equations

$$\begin{aligned} \dot{\lambda}_E &= -\frac{\partial H}{\partial E} - \sigma^T \frac{\partial g}{\partial E} - \mu \frac{\partial C_1}{\partial E} \\ \dot{\lambda}_h &= -\frac{\partial H}{\partial h} - \sigma^T \frac{\partial g}{\partial h} - \mu \frac{\partial C_1}{\partial h} \\ \dot{\lambda}_\gamma &= -\frac{\partial H}{\partial \gamma} - \sigma^T \frac{\partial g}{\partial \gamma} - \mu \frac{\partial C_1}{\partial \gamma} \\ \dot{\lambda}_x &= -\frac{\partial H}{\partial x} - \sigma^T \frac{\partial g}{\partial x} - \mu \frac{\partial C_1}{\partial x} \end{aligned} \tag{21}$$

where σ_i, $i = 1, \ldots, 4$ and μ are multipliers associated with constraints $g_i \le 0$, $i = 1, \ldots, 4$ and $C_1 \le 0$ [C_1 as given in Eq. (18)], respectively. On time intervals where constraint Eq. (10) is not active [i.e., $C_0(E, h, \gamma, x) < 0$], multiplier μ is identically zero

$$\mu = 0 \quad \text{if} \quad C_0(t) < 0 \tag{22}$$

On these intervals multipliers σ_i, $i = 1, \ldots, 4$ are determined at each instant of time from the Kuhn-Tucker conditions[8-11] applied to the finite dimensional parameter optimization problem

$$(\delta, n) = \arg \min_{g \le 0} H \tag{23}$$

At times where state constraint (10) is active [i.e., $C_0(E, h, \gamma, x) = 0$], multipliers σ and μ are determined from the Kuhn-Tucker conditions applied to the finite dimensional parameter optimization problem

$$(\delta, n) = \arg \min_{g \le 0,\, C_1 \le 0} H \tag{24}$$

and components of multiplier vector σ are non-negative along intervals where the associated constraints are active, i.e.

$$\sigma_i \ge 0 \quad \text{if} \quad g_i = 0, \qquad i = 1, \ldots, 4 \tag{26}$$

Note that the optimization problems Eqs. (23) and (24) simply represent the min-Hamiltonian operation required by the PMP.

VI. Possible Control Logics

At each instant of time controls n and δ are determined from the minimum principle given by Eq. (23) in case $C_1 < 0$ and Eq. (24) in case $C_1 = 0$. Since the Hamiltonian H and the constraint functions g and C_1 are smooth functions of their arguments δ and n, the Kuhn-Tucker conditions imply that at the solution point $[\delta^*, n^*]$ the following conditions have to be satisfied at each instant of time:

$$\frac{\partial}{\partial \delta}(H + \sigma^T g + \mu C_1) = 0 \tag{27}$$

$$\frac{\partial}{\partial n}(H + \sigma^T g + \mu C_1) = 0 \tag{28}$$

$$g \le 0 \tag{29}$$

$$C_1 \le 0 \tag{30}$$

$$\sigma \ge 0 \tag{31}$$

$$\mu \ge 0 \tag{32}$$

$$\begin{bmatrix} \Delta\delta \\ \Delta n \end{bmatrix} \begin{bmatrix} \dfrac{\partial^2(H + \sigma^T g + \mu C_1)}{\partial \delta^2} & \dfrac{\partial^2(H + \sigma^T g + \mu C_1)}{\partial \delta \partial n} \\ \dfrac{\partial^2(H + \sigma^T g + \mu C_1)}{\partial n \partial \delta} & \dfrac{\partial^2(H + \sigma^T g + \mu C_1)}{\partial n^2} \end{bmatrix} \begin{bmatrix} \Delta\delta \\ \Delta n \end{bmatrix} \ge 0 \tag{33}$$

for all $(\Delta\delta, \Delta n) \in \boldsymbol{R}^2$ satisfying $(\partial h/\partial \delta)\Delta\delta + (\partial h/\partial n)\Delta n = 0$. Here vector function h contains exactly the active components of the inequality constraints $g \le 0$ and $C_1 \le 0$. The set of active control constraints and the character of the solution of Eqs. (27-33) depends greatly on the direction of the multiplier vector $[\lambda_E, \lambda_h, \lambda_\gamma, \lambda_x]^T$, and through state constraint (10) also on the state itself. The explicit analysis for solving this finite dimensional constrained minimization problem as well as application of the generalized Legendre-Clebsch condition are given in Ref. 12. It is helpful to define

$$n_0 \equiv \frac{\lambda_\gamma}{\lambda_E} \frac{gq}{2v^2 WK} \tag{34}$$

$$n_1 \equiv \frac{\lambda_E}{\lambda_x} \frac{v}{g} \cos^2\gamma \frac{\partial(D_{\max} v/W)}{\partial h} + 2\cos\gamma \tag{35}$$

$$n_2 \equiv \frac{q}{W} \sqrt{\frac{T - vW/g \sin\gamma(v'_{\max} + q/v) - qC_{D0}}{qK}} \tag{36}$$

$$n_3 \equiv \cos\gamma - \frac{\left[\left(\dfrac{\partial D_{\max}}{\partial E}\left(\dfrac{v'_{\max} v}{g} + 1\right) + \dfrac{\partial D_{\max}}{\partial h}\right)\dfrac{g}{W} + v'^2_{\max} + v''_{\max} v\right] v \sin\gamma}{\dfrac{g}{v}(v'_{\max} v + g)\cos\gamma} \tag{37}$$

In both cases, as a consequence of the Kuhn-Tucker conditions, components of multiplier vector σ are zero along intervals where the associated constraint is not active

$$\sigma_i = 0 \quad \text{if} \quad g_i > 0, \qquad i = 1, \ldots, 4 \tag{25}$$

$$\delta_1 \equiv \frac{D_{\max} + \dfrac{vW}{g} \sin\gamma\left(v'_{\max} + \dfrac{g}{v}\right)}{T - D|_{n = n_{\max}} + D_{\max}} \tag{38}$$

Here n_0 is obtained from $\partial H/\partial n = 0$, n_1 solves $\ddot{\lambda}_\gamma \equiv 0$ in the singular case 6b in the Appendix, n_2 is implied by $C_1 = 0$ with $\delta = 1$, and n_3 is required for the singular control case 11b. The expression δ_1 stems from $C_1 = 0$ with $n = n_{\max}$. Then the different possible control logics are shown in the Appendix. A derivation of the results is given in Ref. 12.

VII. Transversality and Corner Conditions

All transversality and corner conditions are given such that the first variation of the cost function Eq. (5) $J = -x(t_f)$ is zero.[8-10] With boundary conditions (11) this yields

$$\lambda_x = -1 \tag{39}$$

In case of final time t_f to be minimized [i.e., cost function Eq. (5) $J = -x(t_f)$ being replaced by $J = t_f$], the associated boundary condition is

$$H(t_f) = 1 \tag{40}$$

The Hamiltonian H is continuous throughout the time interval $[0, t_f]$. At any corner point, say at time t_c, this yields an optimality condition on the switching time t_c, namely

$$H(t_c^+) - H(t_c^-) = 0 \tag{41}$$

Here and later superscripts + and − denote evaluation just right and just left of the time under consideration, respectively. At the beginning, say t_1, of a state constrained arc additional conditions are

$$C_0(t_1) = 0 \tag{42}$$

$$\begin{aligned}
\lambda_E^+ &= \lambda_E^- - l_0 \frac{\partial C_0}{\partial E} \\
\lambda_h^+ &= \lambda_h^- - l_0 \frac{\partial C_0}{\partial h} \\
\lambda_\gamma^+ &= \lambda_\gamma^- - l_0 \frac{\partial C_0}{\partial \gamma} \\
\lambda_x^+ &= \lambda_x^- - l_0 \frac{\partial C_0}{\partial x}
\end{aligned} \tag{43}$$

where l_0 is a constant multiplier. The end, say t_2, of a constrained arc is determined by the continuity of the Hamiltonian. The jump in multipliers in Eq. (43) is implied by the interior point condition Eq. (42).

VIII. Supplementary Optimality Conditions

Along constrained arcs we have the sign conditions[14]

$$\sigma_i \geq 0 \quad \text{on arcs where} \quad g_i = 0 \qquad i = 1, \ldots, 4 \tag{44}$$

$$\mu \geq 0 \quad \text{on arcs where} \quad C_0 = 0 \tag{45a}$$

$$\dot{\mu} \leq 0 \quad \text{on arcs where} \quad C_0 = 0 \tag{45b}$$

Along singular arcs an additional optimality condition is the generalized Legendre-Clebsch condition.[12,13] This condition is already considered in the possible control logics stated in Sec. VI. The explicit analysis is given in Ref. 12.

IX. Switching Structures

Equation (5) is solved for fixed final time Eq. (12) subject to the equations of motion Eqs. (13) and (2-4) and the boundary conditions (11). As a first step only control constraints (14) and (15) and the state constraint (10) are enforced, whereas load factor limits (8) and (9) are neglected. The associated switching structure turns out to be

$$(S1)\ 1-7-11b-7-1$$

where any number i in the sequence refers to case i of the possible control logics listed in the Appendix. The load factor $n = L/W$ increases rapidly near the final time t_f and reaches a maximum value of approximately $n_{\max} = 56.5886$. Mathematically this value is perfectly reasonable, as will be explained heuristically in the next section. To make the solution meaningful from an engineering point of view lower values of $n_{\max}$ have to be enforced. Starting with switching structure $(S1)$ this procedure is done by reducing the load factor limit Eq. (9) in steps

$$|n| \leq n_{\max}, \qquad n_{\max} = 56, 55, \ldots, 5$$

In the process we observe the following switching structures:

$$\begin{aligned}
&(S1)\ 1-7-11b-7-1 && \text{for } n_{\max} \in [56.6, \infty] \\
&(S2)\ 1-7-11b-7-1-3 && \text{for } n_{\max} \in [32.7, 56.5] \\
&(S3)\ 1-7-11b-7-1-3-5 && \text{for } n_{\max} \in [22.7, 32.6] \\
&(S4)\ 1-7-11b-9-7-1-3-5 && \text{for } n_{\max} \in [20.8, 22.6] \\
&(S5)\ 1-7-11b-9-3-5 && \text{for } n_{\max} \in [18.2, 20.7] \\
&(S6)\ 1-7-11b-9-5 && \text{for } n_{\max} \in [5.0, 18.1]
\end{aligned} \tag{46}$$

X. Large Load Factors near Final Time

Figure 3 shows the time history of the load factor along the solution without the bounds Eqs. (8) and (9) (i.e., $n_{\max} = \infty$). It may be helpful to provide some explanation for why the peak-value occurs at the final time and how the peak-value depends on the boundary conditions. To this end, suppose the conditions (11e-11g) are replaced with

$$E(t_f) = E_f = \frac{v_{\max}(h_f)^2}{2g} + h_f \tag{47}$$

$$h(t_f) = h_f = 9000 \tag{48}$$

$$\lambda_\gamma(t_f) = 0 \tag{49}$$

i.e., the prescribed final state lies on the dynamic pressure limit and the final flight path angle is free. Then numerical calculations show that the switching structure associated with the solution of this problem is given by switching structure $(S1)$ of the previous section with the last two arcs deleted. Now, if boundary condition (47) is replaced by

$$E(t_f) = E_f - \Delta E \tag{50}$$

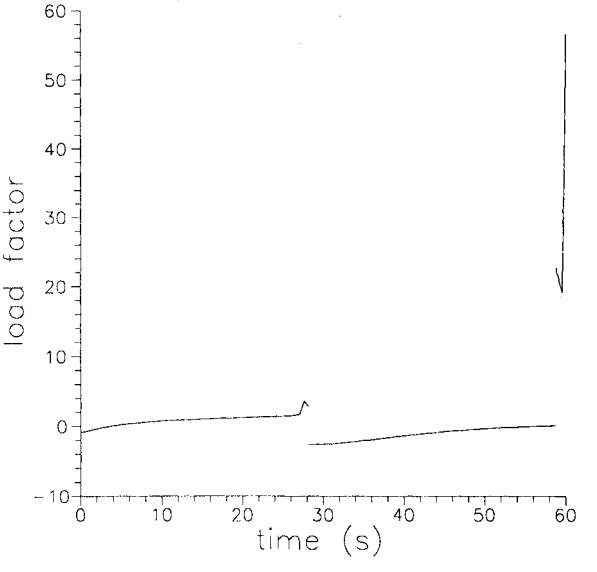

Fig. 3 Load factor n vs time t for $n_{\max} = \infty$ [switching structure $(S1)$].

for some $\Delta E > 0$, then, if the load factor is unbounded, the "optimal maneuver" for the aircraft would be to fly exactly as in the solution of the previous case (i.e., boundary conditions (47–49) until $E(t_f) = E_f$ is reached and then to impulsively apply a high load factor $n \to \infty$ on an infinitesimal time interval $[t_f, t_f + \delta t_f]$, $\delta t_f \to 0$, such that the energy drops instantaneously to the prescribed value $E_f - \Delta E$. By noting that, in the dynamical equations, the load factor appears linearly in the $\dot{\gamma}$-equation and quadratically in the $\dot{E}$-equation, we expect that along this infinitesimal arc $\delta E \sim n^2 \delta t$, whereas $\delta\gamma \sim n\delta t$. Hence, with n and δt_f such that $\delta E = -\Delta E$ we expect $\delta\gamma \to 0$ for $n \to \infty$, and the flight-path angle does not change along this arc.

If the final flight-path angle is prescribed at a value different from the natural one, i.e., Eq. (49) is replaced by

$$\gamma(t_f) = \gamma_{\text{free}} + \Delta\gamma, \qquad \Delta\gamma \neq 0 \tag{51}$$

Then the dissipation of energy turns into a gradual process extending over a nonzero time interval, and the load factor remains finite. Paradoxically, nonzero $\Delta\gamma$ results in a smaller peak value load-factor than does $\Delta\gamma = 0$.

XI. Numerical Approach

The switching structure, that is, the sequence of different control logics that actually solves a problem is not known in advance. For a given problem it has to be found by numerical experiments. Assuming a certain switching structure, the state and costate equations along with the boundary conditions, transversality conditions, and corner conditions implied by the assumed switching structure yield a multipoint boundary value problem (MPBVP). As an example case a schematic representation of the MPBVP associated with switching structure (*S*6) is given in Fig. 4. By inspection it is clear that the trajectory can be determined by simple forward integration if all parameters $E(0)$, $h(0)$, $\gamma(0)$, $x(0)$, $\lambda_E(0)$, $\lambda_h(0)$, $\lambda_\gamma(0)$, $\lambda_x(0)$, l_0, Δt_1, Δt_2, Δt_3, Δt_4, and Δt_5 are known. Basically, the numerical problem is to determine these 14 parameters such that all 14 conditions (numbered 1–14 in Fig. 4) are satisfied. This root finding problem is solved using routine ZSCNT of the IMSL subroutine library (version 9.2). In practice, forward integration causes the associated boundary value problem to be very badly conditioned. A remedy is to consider t_3 as a new initial point and generate trajectories by successively integrating backward and forward, starting at switching time t_3, respectively. In an obvious way this generates a new set of parameters $E(t_3)$, $h(t_3)$, $\gamma(t_3)$, $x(t_3)$, $\lambda_E(t_3)$, $\lambda_h(t_3)$, $\lambda_\gamma(t_3)$, $\lambda_x(t_3)$, l_0, Δt_1, Δt_2, Δt_3, Δt_4, and Δt_5 along with the conditions numbered 1–14 in Fig. 4. Noting that conditions 6, 8, and 10 in Fig. 4 can equivalently be enforced at time t_3, three unknowns, say $E(t_3)$, $\lambda_h(t_3)$, and $\lambda_\gamma(t_3)$ can be expressed in terms of the remaining 12

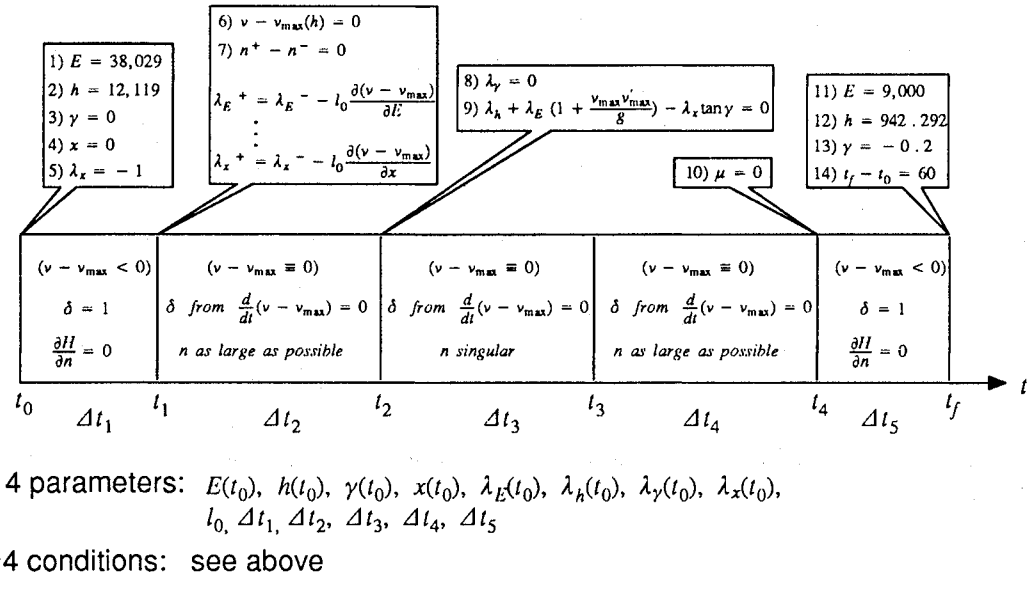

Fig. 4 Schematic representation of the boundary value problem associated with switching structure (*S*6).

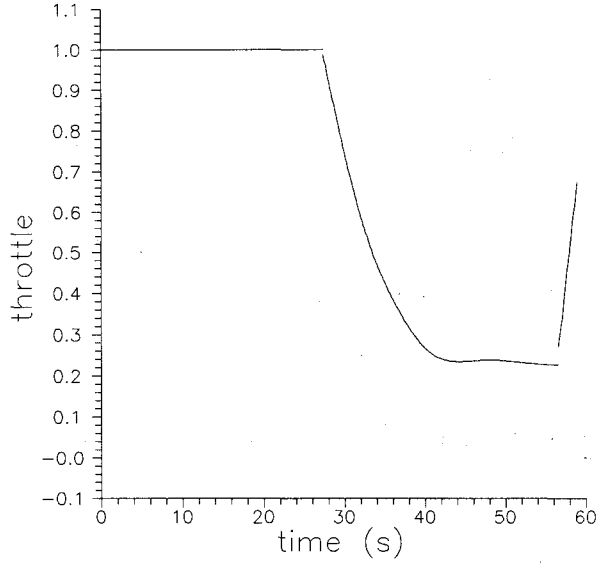

Fig. 5 Throttle η vs time t for $n_{\max} = 10$ [switching structure (*S*6)].

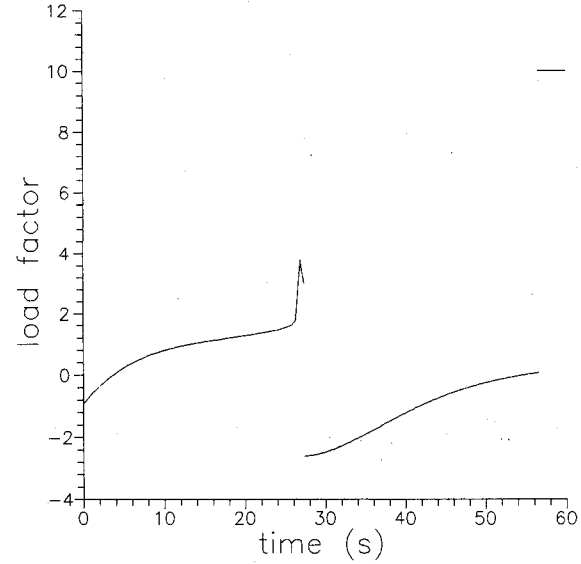

Fig. 6 Load factor n vs time t for $n_{\max} = 10$ [switching structure (*S*6)].

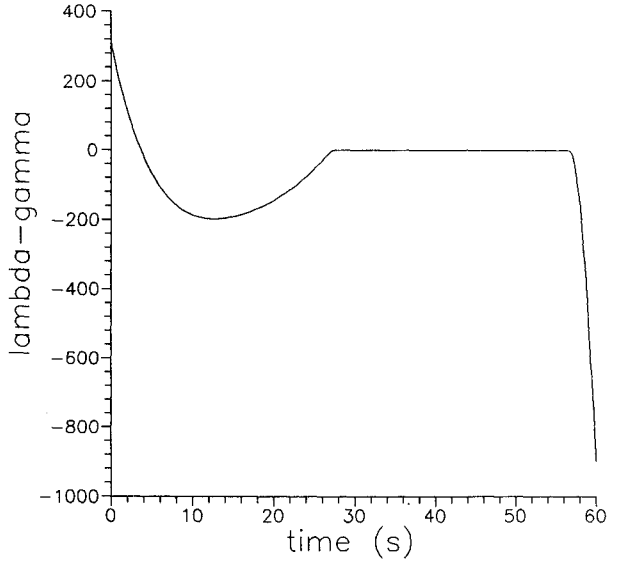

Fig. 7 Costate λ_γ vs time t for $n_{max} = 10$ [switching structure ($S6$)].

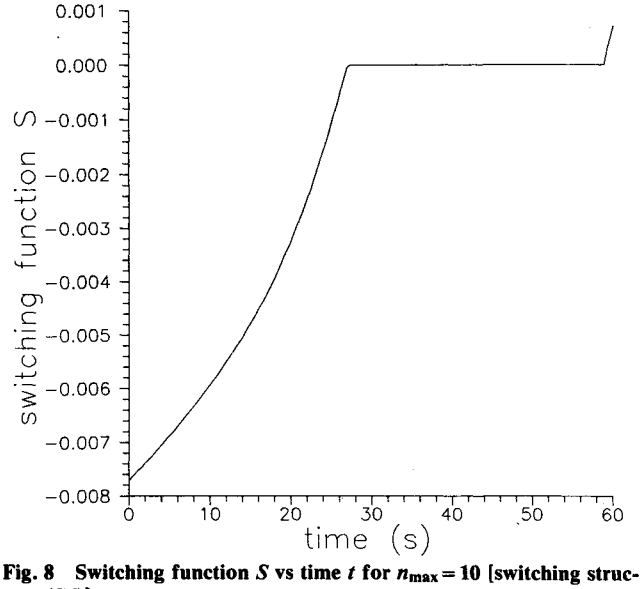

Fig. 8 Switching function S vs time t for $n_{max} = 10$ [switching structure ($S6$)].

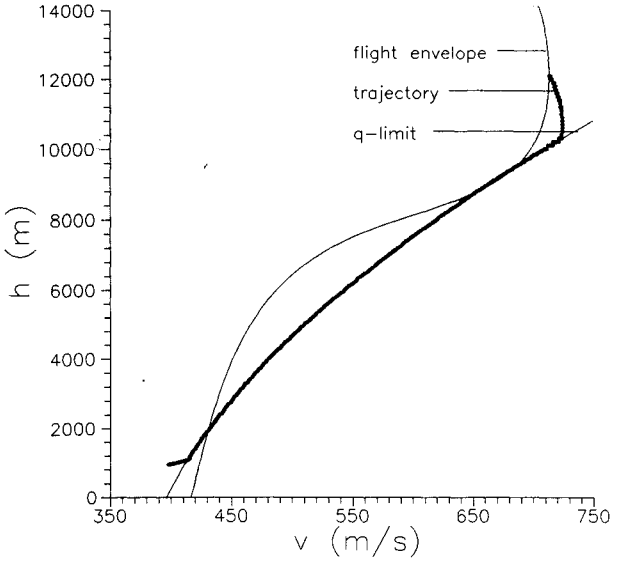

Fig. 9 Altitude-velocity chart for a typical extremal.

Table 4 Lengths of subarcs in seconds for selected trajectories associated with switching structures ($S1$)-($S6$)

n_{max}	Δt_1	Δt_2	Δt_3	Δt_4	Δt_5	Δt_6	Δt_7	Δt_8
free	27.622	0.525	30.614	0.796	0.443	—	—	—
34	27.618	0.525	30.686	0.536	0.104	0.530	—	—
23	27.491	0.521	30.539	0.451	0.015	0.515	0.567	—
21	27.449	0.520	30.467	0.420	0.045	0.002	0.506	0.591
20	27.423	0.519	30.412	0.651	0.340	0.654	—	—
10	26.856	0.504	29.231	2.31	1.098	—	—	—

parameters $h(t_3)$, $\gamma(t_3)$, $x(t_3)$, $\lambda_E(t_3)$, $\lambda_x(t_3)$, l_0, Δt_1, Δt_2, Δt_3, Δt_4, and Δt_5. Whereas it is only of minor importance that this reduces the number of parameters and conditions, it is very significant that this substitution ensures that 1) the characteristics of the singular arc, i.e., conditions 8 and 9 in Fig. 4, are satisfied along $[t_2, t_3]$ and 2) the dynamic pressure limit $v - v_{max}(h) = 0$ is satisfied along $[t_1, t_4]$. Note that both points hold true even before the root finding process converges.

XII. Numerical Results

As a general trend it is observed that all trajectories consist of mainly three phases. Phase 1 is the full thrust flight off the dynamic pressure limit (case 1) until dynamic pressure limit is reached. Phase 2 is the rapid descent with dynamic pressure limit active and singular control power (case 11b) until close to prescribed final altitude. Phase 3 is the rapid pitchup maneuver off the dynamic pressure limit with load factor on its upper limit and thrust first full, then zero.

In Table 4, the lengths of each arc in seconds are given for selected solutions with switching structures ($S1$)-($S6$) [compare Eq. (46)]. For the case of $n_{max} = 10$ (switching structure $S6$) time histories for throttle η, load factor n, Lagrange multiplier λ_γ, and switching function $S = \lambda_E(v/W) + \mu(g/W)$ are given in Figs. 5-8, respectively. Figure 9 shows the altitude-velocity chart for this solution.

All switching structures found seem to be of some general nature in the sense that the same switching structures arise if initial or final coordinates of the trajectory are moderately changed. In this context trajectories starting at ground level with speed around takeoff velocity have been calculated for prescribed flight times over 200 s and final conditions as in Eq. (11). For long flight times [over 62 s for initial and final conditions as given in Eq. (11)] the obtained switching structures $S1$-$S6$ do not solve the problem. (Thrust oversaturates at the beginning of the singular thrust arc.) The correct switching structure for long flight times has not yet been found.

XIII. Summary

Range optimal trajectories for an aircraft flying in the vertical plane are synthesized in the presence of a dynamic pressure limit (state inequality constraint) and a load factor limit (control inequality constraint). The trajectories start at the dash-point and end at prescribed final states inside the level-flight envelope, off the dynamic pressure limit. For a fixed flight time of 62 s the effect of the load factor limit on the resulting optimal switching structure is investigated. Six different switching structures are obtained with singular control along state constrained arcs always playing an important role. The switching structures identified in this paper appear to be of a general nature and are not restricted to the specific boundary conditions considered here. For long flight times greater than 62 s, however, and for the boundary conditions prescribed in this paper the optimal switching structure has not yet been found.

Appendix: Possible Control Logics

Case 1: Constraint equation (10) is not active, $\lambda_E < 0$, $n_0 \in [-n_{max}, +n_{max}]$:

$$\delta = 1$$

$$n = n_0$$
$$\sigma_1 = 0$$
$$\sigma_2 = -\lambda_E(T - D + D_{\max})\frac{v}{W} \tag{A1}$$
$$\sigma_3 = 0$$
$$\sigma_4 = 0$$
$$\mu = 0$$

Case 2: Constraint equation (10) is not active, $\lambda_E < 0$, $n_0 < -n_{\max}$:

$$\delta = 1$$
$$n = -n_{\max}$$
$$\sigma_1 = 0$$
$$\sigma_2 = -\lambda_E(T - D + D_{\max})\frac{v}{W} \tag{A2}$$
$$\sigma_3 = \frac{\partial H}{\partial n}$$
$$\sigma_4 = 0$$
$$\mu = 0$$

Case 3: Constraint equation (10) is not active, $\lambda_E < 0$, $n_0 > n_{\max}$:

$$\delta = 1$$
$$n = n_{\max}$$
$$\sigma_1 = 0$$
$$\sigma_2 = -\lambda_E(T - D + D_{\max})\frac{v}{W} \tag{A3}$$
$$\sigma_3 = 0$$
$$\sigma_4 = -\frac{\partial H}{\partial n}$$
$$\mu = 0$$

Case 4: Constraint equation (10) is not active, $\lambda_E > 0$, $\lambda_\gamma > 0$:

$$\delta = 0$$
$$n = -n_{\max}$$
$$\sigma_1 = \lambda_E(T - D + D_{\max})\frac{v}{W}$$
$$\sigma_2 = 0 \tag{A4}$$
$$\sigma_3 = \frac{\partial H}{\partial n}$$
$$\sigma_4 = 0$$
$$\mu = 0 \tag{A5}$$

Case 5: Constraint equation (10) is not active, $\lambda_E > 0$, $\lambda_\gamma < 0$:

$$\delta = 0$$
$$n = n_{\max}$$
$$\sigma_1 = \lambda_E(T - D + D_{\max})\frac{v}{W}$$
$$\sigma_2 = 0 \tag{A6}$$
$$\sigma_3 = 0$$
$$\sigma_4 = -\frac{\partial H}{\partial n}$$
$$\mu = 0 \tag{A7}$$

Case 6: Constraint equation (10) is not active, $\lambda_E > 0$, $\lambda_\gamma = 0$.

In this case the controls are not determined uniquely by the minimum principle. Pointwise occurrence of this situation can be ignored. Assuming that $\lambda_\gamma \equiv 0$ on some nonzero time interval yields control n after differentiating twice (singular control of first-order). Two cases have to be distinguished, namely $\lambda_x = 0$ and $\lambda_x \neq 0$.

Case 6a: Constraint equation (10) is not active, $\lambda_E > 0$, $\lambda_\gamma = 0$, and $\lambda_x = 0$.

Then necessarily $\lambda_h \neq 0$ and

$$\delta = 0$$
$$\lambda_\gamma = 0$$
$$\cos\gamma = 0$$
$$n = 0$$
$$\sigma_1 = \lambda_E(T - D + D_{\max})\frac{v}{W} \tag{A8}$$
$$\sigma_2 = 0$$
$$\sigma_3 = 0$$
$$\sigma_4 = 0$$
$$\mu = 0 \tag{A9}$$

The generalized Legendre-Clebsch condition[12,13] implies

$$\sin\gamma > 0 \quad \text{if} \quad \lambda_h < 0$$
$$\sin\gamma < 0 \quad \text{if} \quad \lambda_h > 0$$

Case 6b: Constraint equation (10) is not active, $\lambda_E > 0$, $\lambda_\gamma = 0$, and $\lambda_x \neq 0$:

$$\delta = 0$$
$$\lambda_\gamma = 0$$
$$\lambda_h - \lambda_x \tan\gamma = 0$$
$$n = n_1$$
$$\sigma_1 = \lambda_E\,(T - D + D_{\max})\frac{v}{W} \tag{A10}$$
$$\sigma_2 = 0$$
$$\sigma_3 = 0$$
$$\sigma_4 = 0$$
$$\mu = 0 \tag{A11}$$

The generalized Legendre-Clebsch condition implies $\lambda_x < 0$.

The case $\lambda_E \equiv 0$, $\lambda_\gamma \equiv 0$ can be excluded. The case $\lambda_E \equiv 0$, $\lambda_\gamma \neq 0$ leads to first-order singular control in throttle δ, which is rejected as nonoptimal by the generalized Legendre-Clebsch condition.

Case 7: Constraint equation (10) is active, $\lambda_E + \mu(g/v) < 0$, $\lambda_\gamma < 0$:

$$\delta = 1$$
$$n = n_2$$
$$\sigma_1 = 0$$
$$\sigma_2 = -\left(\lambda_E + \mu\frac{g}{v}\right)(T - D + D_{\max})\frac{v}{W} \tag{A12}$$
$$\sigma_3 = 0$$
$$\sigma_4 = 0$$
$$\mu = \frac{\lambda_\gamma}{n}\frac{q}{2Kv W} - \lambda_E\frac{v}{g} \tag{A13}$$

Case 8: Constraint equation (10) is active, $\lambda_E + \mu(g/v) < 0$, $\lambda_\gamma > 0$:

$$\delta = 1$$

$$n = -n_2$$
$$\sigma_1 = 0$$
$$\sigma_2 = -\left(\lambda_E + \mu\frac{g}{v}\right)(T - D + D_{\max})\frac{v}{W} \tag{A14}$$
$$\sigma_3 = 0$$
$$\sigma_4 = 0$$
$$\mu = \frac{\lambda_\gamma}{n}\frac{q}{2KvW} - \lambda_E\frac{v}{g} \tag{A15}$$

The case where constraint equation (10) is active, $\lambda_E + \mu(g/v) > 0$ and $\lambda_\gamma \neq 0$ can be excluded. The case where constraint equation (10) is active, $\lambda_E + \mu(g/v) = 0$ and $\lambda_\gamma = 0$ is treated later.

Case 9: Constraint equation (10) is active, $\lambda_E + \mu(g/v) = 0$, $\lambda_\gamma < 0$:

$$\delta = \delta_1 \text{ (from } C_1 = 0 \text{ with } n = n_{\max})$$
$$n = n_{\max}$$
$$\sigma_1 = 0$$
$$\sigma_2 = 0 \tag{A16}$$
$$\sigma_3 = 0$$
$$\sigma_4 = -\lambda_\gamma\frac{g}{v}$$
$$\mu = -\lambda_E\frac{v}{g} \tag{A17}$$

Case 10: Constraint equation (10) is active, $\lambda_E + \mu(g/v) = 0$, $\lambda_\gamma > 0$:

$$\delta = \delta_1 \text{ (from } C_1 = 0 \text{ with } n = n_{\max})$$
$$n = -n_{\max}$$
$$\sigma_1 = 0$$
$$\sigma_2 = 0 \tag{A18}$$
$$\sigma_3 = \lambda_\gamma\frac{g}{v}$$
$$\sigma_4 = 0$$
$$\mu = -\lambda_E\frac{v}{g} \tag{A19}$$

Case 11: Constraint equation (10) is active, $\lambda_E + \mu(g/v) = 0$, $\lambda_\gamma = 0$.

In this case the controls are not determined uniquely by the minimum principle. Pointwise occurrence of this situation can be ignored. Assuming that $\lambda_\gamma \equiv 0$ on some nonzero time interval additional information has to be obtained from differentiating identity $\lambda_\gamma \equiv 0$ (singular control). Two cases have to be distinguished, namely $\lambda_x = 0$ and $\lambda_x \neq 0$.

Case 11a: Constraint equation (10) is active, $\lambda_E + \mu(g/v) = 0$, $\lambda_\gamma = 0$, $\lambda_x = 0$.

In this case we have two possible control logics, namely

$$\delta = \frac{D_{\max} + \frac{vW}{g}\sin\gamma\left(v'_{\max} + \frac{g}{v}\right)}{T - D|_{n=\cos\gamma} + D_{\max}}$$
$$\lambda_\gamma = 0$$
$$\sin\gamma = 0$$
$$n = \cos\gamma$$
$$\sigma_1 = 0 \tag{A20}$$
$$\sigma_2 = 0$$
$$\sigma_3 = 0$$
$$\sigma_4 = 0$$
$$\mu = -\lambda_E\frac{v}{g} \tag{A21}$$

and

$$\delta = \frac{D_{\max} + \frac{vW}{g}\sin\gamma\left(v'_{\max} + \frac{g}{v}\right)}{T - D + D_{\max}}$$
$$\lambda_\gamma = 0$$
$$\lambda_h + \lambda_E\left(1 + \frac{v'_{\max}v}{g}\right) = 0$$
$$\sin\gamma = 0$$
$$n = \cos\gamma$$
$$\sigma_1 = 0 \tag{A22}$$
$$\sigma_2 = 0$$
$$\sigma_3 = 0$$
$$\sigma_4 = 0$$
$$\mu = -\lambda_E\frac{v}{g} \tag{A23}$$

Here, Eqs. (A20) represent singular control of first-order (in control n). Equation (A22) represents a case of infinite-order singular control. In this case, control n is undetermined. Every control function of time $n(t)$ is admissible, as long as it leads to state/costate time histories that satisfy all boundary, transversality, and switching conditions.

Case 11b: Constraint equation (10) is active, $\lambda_E + \mu(g/v) = 0$, $\lambda_\gamma = 0$, and $\lambda_x \neq 0$.

Then necessarily $\cos\gamma \neq 0$ and

$$\delta = \frac{D_{\max} + \frac{vW}{g}\sin\gamma\left(v'_{\max} + \frac{g}{v}\right)}{T - D|_{n \text{ as below}} + D_{\max}}$$
$$\lambda_\gamma = 0$$
$$\lambda_h - \lambda_x\tan\gamma + \lambda_E\left(1 + \frac{v'_{\max}v}{g}\right) = 0$$
$$n = \left(1 - \frac{v'_{\max}v}{g}\right) = \cos\gamma \tag{A24}$$
$$\sigma_1 = 0$$
$$\sigma_2 = 0$$
$$\sigma_3 = 0$$
$$\sigma_4 = 0$$
$$\mu = -\lambda_E\frac{v}{g} \tag{A25}$$

The generalized Legendre-Clebsch condition implies $\lambda_x < 0$.

Case 12: Constraint equation (10) is active, $\lambda_E + \mu(g/v) \neq 0$, $\lambda_\gamma = 0$.

Then necessarily $\cos\gamma \neq 0$ and

$$\delta = 0$$
$$\lambda_\gamma = 0$$
$$D_{\max}\frac{g}{W} + v\sin\gamma\left(v'_{\max} + \frac{g}{v}\right) = 0$$
$$n = n_3 \tag{A26}$$
$$\sigma_1 = \left(\lambda_E + \mu\frac{g}{v}\right)(T - D + D_{\max})\frac{v}{W}$$

$$\sigma_2 = 0$$

$$\sigma_3 = 0$$

$$\sigma_4 = 0$$

$$\mu = \frac{\lambda_h - \lambda_x \tan\gamma}{v'_{\max} + \frac{g}{v}} \tag{A27}$$

Acknowledgments

The research that led to the results presented in this paper was supported in part by NASA Grants NAG-1-946 and NAG-1-1244, in part by DARPA Contract F 49620-87-C-0116, and in part by NASA Contract NAS1-18935. The authors greatly appreciate various comments and suggestions from John A. Burns and the late Henry J. Kelley.

References

[1]Shinar, J., Well, K. H., and Jaermark, B., "Near-Optimal Feedback Control for Three-Dimensional Interceptions," *Proceedings of the International Council of the Aeronautical Sciences,* September 1986, pp. 161–171 (ICAS Paper 86-5.1.3).

[2]Grimm, G., "A Numerical Approach for On-Line Guidance of Aircraft," *Proceedings of the IEEE Conference on Decision and Control* (Athens, Greece), 1986, pp. 683–687.

[3]Grimm, W., and Hiltmann, P., "Direct and Indirect Approach for Real-Time Optimization of Flight Paths," *Lecture Notes in Control and Information Sciences,* Vol. 95, edited by R. Bulirsch et al., Springer Verlag, Berlin, 1986, pp. 190–206.

[4]Shankar, U. J., Cliff, E. M., and Kelley, H. J., "Singular Perturbation Analysis of Optimal Climb-Cruise-Dash," *Proceedings of the AIAA Guidance, Navigation, and Control Conference* (Monterey, CA), AIAA, New York, 1987, pp. 1087–1095.

[5]Calise, A. J., and Moerder, D. D., "Singular Perturbation Techniques for Real-Time Aircraft Trajectory Optimization and Control," NASA CR-3597, Aug. 1982.

[6]Kumar, R. R., Seywald, H., Cliff, E. M., and Kelley, H. J., "3-D Air-to-Air Missile Trajectory Shaping Study," *Proceedings of the AIAA Guidance, Navigation, and Control Conference* (Boston, MA), AIAA, Washington, DC, 1989, pp. 470–481.

[7]Kumar, R. R., Seywald, H., and Cliff, E. M., "Near Optimal 3-D Guidance Against a Maneuvering Target," *Proceedings of the AIAA Guidance, Navigation, and Control Conference* (Boston, MA), AIAA, Washington, DC, 1989, pp. 482–495.

[8]Bryson, A. E., and Ho, Y. C., *Applied Optimal Control,* Hemisphere, New York, 1975.

[9]Lee, E. B., and Markus, L., *Foundations of Optimal Control Theory,* Robert E. Krieger Publishing, Malabar, FL, 1986.

[10]Neustadt, L. W., *Optimization: A Theory of Necessary Conditions,* Princeton Univ. Press, Princeton, NJ, 1976.

[11]Wouk, A., *A Course of Applied Functional Analysis,* Wiley, New York, 1976.

[12]Seywald, H., "Optimal Control Problems with Switching Points," NASA CR-4393, Sept. 1991.

[13]Goh, B. S., "Necessary Conditions for Singular Extremals Involving Multiple Control Variables," *SIAM Journal of Control,* Vol. 4, No. 4, 1966, pp. 716–731.

[14]Jacobson, D. H., Lele, M. M., and Speyer, J. L., "New Necessary Conditions of Optimality for Control Problems with State-Variable Inequality Constraints," *Journal of Mathematical Analysis and Applications,* Vol. 35, No. 2, 1971, pp. 255–284.